Transactions of the Materials Research Society of Japan 29 [8] 3759-3762 (2004)

Sorption and Diffusion in Nanoscale Molecular Cavity in Polymer Crystals Studied by Molecular Dynamics Simulation

Yoshinori Tamai and Mitsuhiro Fukuda*
Department of Applied Physics, Faculty of Engineering, University of Fukui
3-9-1 Bunkyo, Fukui 910-8507 JAPAN
Fax: 81-776-27-8032, e-mail: tamai@polymer.apphy.fukui-u.ac.jp
*Textile Materials Science Laboratory, Hyogo University of Teacher Education
942-1 Shimokume, Yashiro-cho, Hyogo 673-1494 JAPAN
Fax: 81-795-44-2189, e-mail: mifukuda@life.hyogo-u.ac.jp

The cavity structure in the polymorphs of crystalline syndiotactic polystyrene was investigated using a molecular dynamics simulation. The size, shape, and connectivity of the cavities and the sorption and diffusion behaviors of gases in the cavity were investigated in detail. Cluster analysis of the free volume in the crystals clearly reveals the cavity structures: large individual holes are in an orderly manner connected by narrow channels. We call such a cavity structure, a "molecular cavity". The cavity structures were reflected by the anisotropy of diffusion. Such crystals, which have a molecular cavity, could be used as a separation material with significantly high permselectivity. The cavity size is large enough for a molecule to permeate, and the regularity of the cavity structure certifies a precise separation.
Key words: molecular dynamics, simulation, polymer, crystal, membrane

1. INTRODUCTION

Syndiotactic polystyrene (s-PS) is known for its unusual crystal polymorphism [1]-[8]. There are four main polymorphs for s-PS, i.e., the α, β, γ, and δ forms. The α and β forms have the all *trans* (TTTT) conformation. The δ form is a clathrate compound with various guests, e.g., toluene, iodine, and 1,2-dichloroethane. The emptied δ_e form can be obtained by the extraction of the solvent molecules from the δ form. The δ form is quite stable below 400 K and transformed into the γ form at higher temperature. The main-chain conformation of the δ, δ_e, and γ forms is s(2/1)2 helical (TTGG). The atomic coordinate data, which were determined by an X-ray diffraction experiment, suggested the presence of nanopores in the δ_e form [8]. The sorption experiments also imply the existence of molecular cavities which have a significant selectivity for particular substances [9]-[13]. In the α form, on the other hand, a one-dimensional diffusion path, through which gas molecules effectively permeate, is expected to exist by a permeation experiment [14].

In a previous study [15], we performed a molecular dynamics (MD) simulation for the polymorphs of s-PS; the size, shape, and connectivity of the cavities in the crystals were elucidated. Cluster analysis of the free volume in the δ_e form clearly reveals the cavity structure; large individual holes are in an orderly manner connected by narrow channels. We call such a cavity structure a "molecular cavity" [15,16]. In contrast, a capillary-like cavity structure was clearly found in the α form. The efficiency of the gas diffusion in the capillary was much higher. The anisotropy of diffusion becomes more significant for the larger size gases, whose diffusion in the α form can be effectively described by a one-dimensional transport [17].

In this paper, the diffusion behavior and solubility of various gases in the molecular cavity were simulated. The applicability of the concept of the molecular cavity to high performance separation membranes is examined.

2. SIMULATION DETAILS

The initial structures of the crystals were generated on the basis of the X-ray diffraction experiments [7,8]. An MD unit cell contains 2x2x8 and 3x4x6 crystal units for the α and δ_e forms, respectively; the total number of atoms is 9,216 for both crystal forms. The potential model and the procedure for the MD simulation are the same as those used in previous studies [15,17]. The three-dimensional periodic boundary condition was applied. The crystal was modeled as a single crystal in which the monomer units are infinitely connected along the c-axis. The bonded interactions of the bond angle, torsion angle, and improper torsion angle and the nonbonded interactions of Lennard-Jones and Coulomb were included in the potential function. The bond lengths were constrained by the SHAKE method. The potential parameters were taken from the all-atom force field, AMBER [18]. The potential parameters for the gases were taken from the literature. The long-range nonbonded interactions were smoothly cut off at 14 Å. The temperature and pressure tensors were controlled by the Nosé [19] and Parrinello-Rahman [20] methods. The equations of motion were solved by a variant of the Verlet algorithm with a time step of 1 fs.

The MD simulations were first performed for 150 ps at 300 K under ambient pressure. The temperature was then increased to 500 K or decreased to 250 K in 50 K interval steps. The equilibration run of 20 ps, followed by the sampling run of 100 ps, was performed at each temperature. Twenty gas molecules were then inserted into the cavities of the crystal at each temperature.

Long-time simulation runs of up to 5 ns were performed for each system, which contained He, Ne, Ar, O_2, N_2, CO_2, or CH_4. The diffusion process of the gases was analyzed in detail. The solubility of the gases was calculated by the particle insertion method [15]. The excluded volume map sampling (EVMS) was used to raise the efficiency. A total of 100,000 insertion trials of the test molecules were attempted only for the nonexcluded volume of the configuration. The samplings were averaged over 20 configurations.

A cluster machine with 28 Intel processors was used for the simulation along with the molecular simulation program PAMPS coded and developed by one of the authors (Y.T.).

3. RESULTS AND DISCUSSION

3.1 Cavity structures

The accessible region in the crystal for a probe of radius R_c was evaluated by a previously described method [15]. Fig. 1 shows one of the continuous accessible regions for a probe of R_c = 0.7 and 0.6 Å for the α and δ_e forms, respectively. The R_c values were determined such that the accessible clusters steeply decrease at that length with increasing R_c [15]. Note that only one representative continuous cluster is shown for each crystal form; many other clusters like this exist in the system. In the α form, the moderate size cavities are continuously connected in straight lines along the c-axis. The cavities form a nanoscale capillary in the crystal. In the δ_e form, on the other hand, the large flat cavities of full 10 Å length are stacked in the c-axial direction. We call such a cavity structure a "molecular cavity", which is represented by a nanoscale cavity with regular size, regular shape, and ordered connectivity [15,16]. The distribution of the accessible volume was analyzed in detail in a previous paper [15].

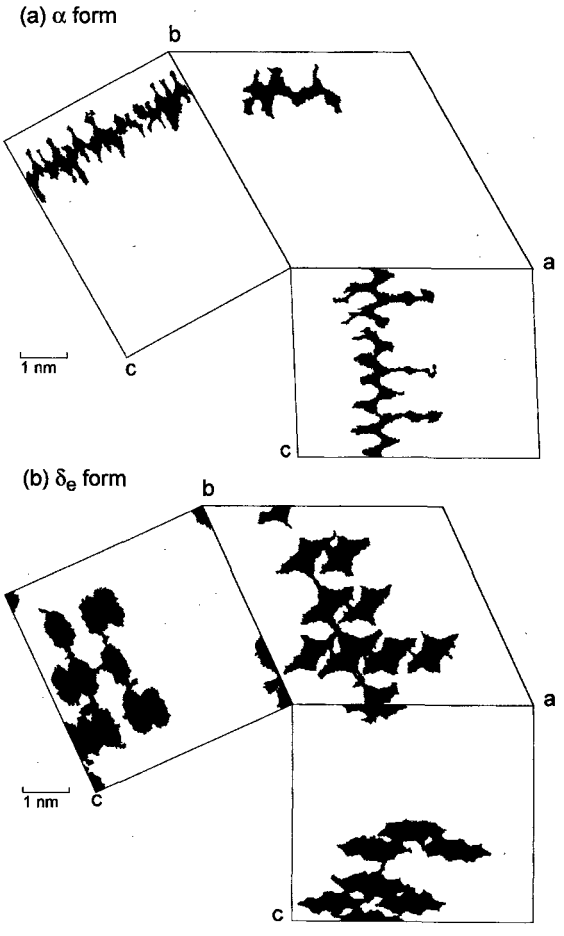

Fig. 1 Projections of one of the continuous accessible regions for a probe of radius R_c: (a) α form for R_c = 0.7 Å and (b) δ_e form for R_c = 0.6 Å.

3.2 Diffusion of gases

The diffusion behavior of each gas molecule in the crystal was simulated. Fig. 2 shows the displacement of one of the penetrant molecules in each crystal. Since the mobility is comparable between Ar in the α form at 300 K and Ne in the δ_e form at 400 K, we compare these two. The diffusion process consists of the vibrational motion in a cavity and the jumping motion between cavities. Both the amplitude of oscillation and the jump distance are significantly long in the δ_e form. On the other hand, the short-distance jumps of the gas molecule are frequently observed in the α form. The difference in the cavity structure is obviously reflected on the diffusion behavior.

Fig. 3 shows the mean-square displacement (MSD), which was separately calculated along each crystal axis and averaged over 20 gas molecules. The marked anisotropy of diffusion is observed. In the α form, the diffusion process is effectively one-dimensional; the gas molecule diffuses along the capillary c-axis. The fast one-dimensional gas transport in the molecular capillary was reported in a previous paper [17]. In the δ_e form,

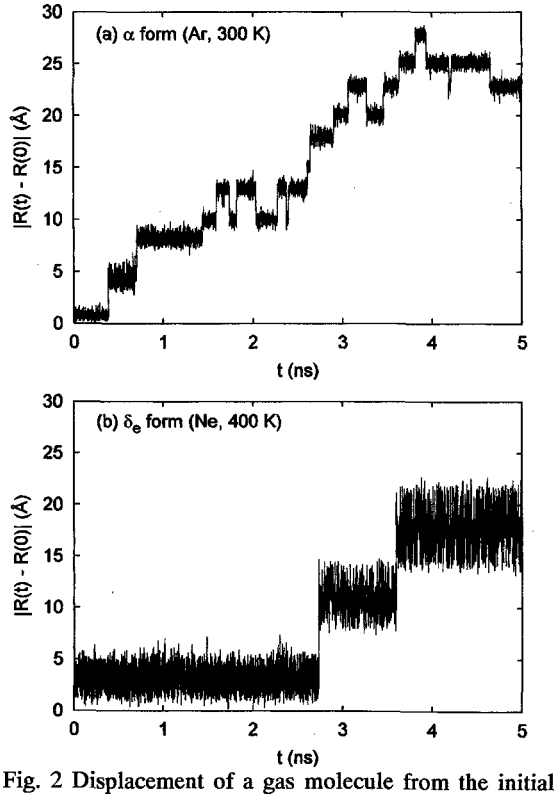

Fig. 2 Displacement of a gas molecule from the initial position in the s-PS crystal: (a) Ar in the α form at 300 K, (b) Ne in the δ_e form at 400 K.

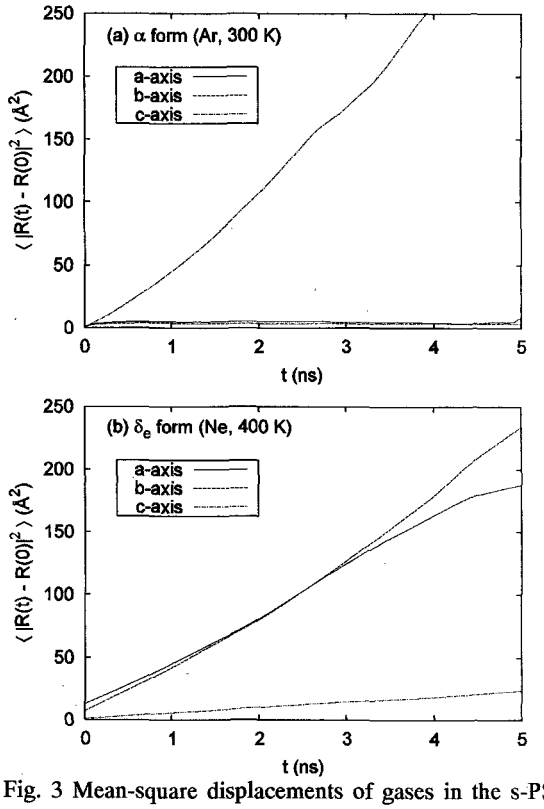

Fig. 3 Mean-square displacements of gases in the s-PS crystal: (a) Ar in the α form at 300 K, (b) Ne in the δ_e form at 400 K.

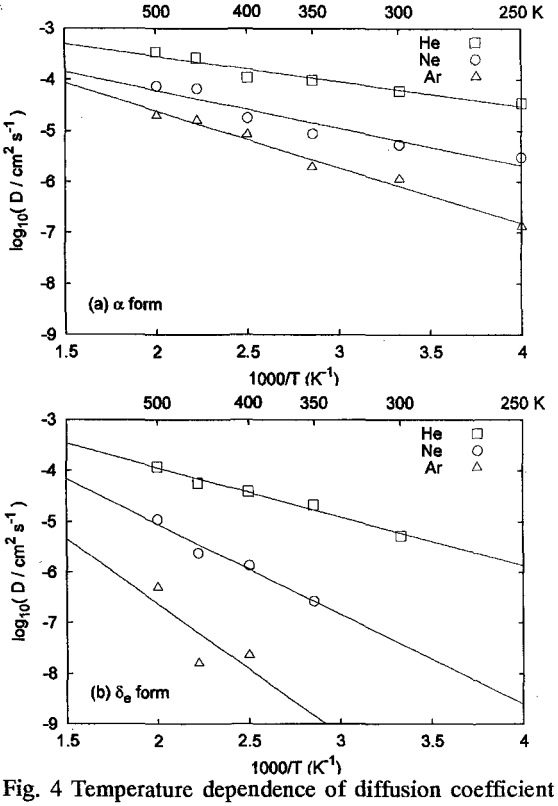

Fig. 4 Temperature dependence of diffusion coefficient of the rare gases in crystalline s-PS: (a) α form, (b) δ_e form.

the main diffusion direction is the a- and b-axes. As discussed in a previous paper [15], the main diffusion pathway in the δ_e form is the <101> direction. The jump distances of the gas are 8.7 Å and 3.9 Å for a- and c-axial directions, respectively, which can be estimated from the crystal periodicity (half values of the edge lengths *a* and *c*, respectively). Because the MSD is proportional to the square of the jump distance, the MSD along the a-axis is expected to be 5 times that along the c-axis. The jumping motion along the b-axis was also observed; the diffusion path along the b-axis is seen in Fig. 1(b). Since the jump distance along this path is long, the MSD along b-axis becomes large, in spite of the low jump probability.

The diffusion coefficient *D* was calculated from the slope of the MSD. The temperature dependence of the diffusion coefficients is shown in Fig. 4. The *D* values satisfactorily obey the Arrhenius law. The activation energy E_a was estimated from the slope of the figure. The E_a values of He, Ne, and Ar in the α form are 9.3, 14.0, and 21.1 kJ/mol, respectively, and those in the δ_e form are 18.4, 34.0, and 49.0 kJ/mol, respectively. Since a molecular size capillary exists in the α form, the activation energy is very small. As a consequence of this fact, the jump probability becomes high; the frequent jump motion is clearly seen in Fig. 2(a). The transport of gas in the α form is very effective. In the δ_e form, the *D* values significantly vary with temperature. Therefore, the diffusion of gases is controllable by the temperature. The effect of penetrant size on the diffusion coefficient is quite remarkable in the δ_e form than that in the α form. Because the jumping motion between two cavities is governed by a very narrow channel in the δ_e form, the size effect is higher in this form.

3.3 Solubility and Permeability

The solubility of gases into the molecular cavity is also of much interest. The calculated solubilities of gases in the α and δ_e forms at 300 K are listed in Table I. The solubility is affected by two factors: the size and energy effects. It is difficult for the larger gases to dissolve in the typical polymer crystals because, in general, their cavity size is small. If the cavity size is large enough, the larger gases can easily dissolve in the crystal. The solubility of the larger gases becomes higher because the interaction with the host matrix is also high for these gases. In the α form, in which moderate size cavities exist, the solubilities are higher than those expected in the ordinary polymer crystals. The solubilities in the δ_e form are significantly higher, especially for the larger gases, since it contains large cavities.

Table I. Solubility *S* of gas molecules in the s-PS crystals at 300 K in a unit of $cm^3(STP)/cm^3$ atm.

Gas	α form	δ_e form
He	0.019	0.13
Ne	0.025	0.51
Ar	0.022	7.6
O_2	0.015	5.1
N_2	0.0027	3.0
CH_4	0.0063	10.4
CO_2	0.120	58.0

Table II. Diffusion coefficient along c-axis D_c and permeability P of gas molecules in the α form at 300 K.

Gas	D_c	P
He	6.53×10^{-5}	1.2×10^{-6}
Ne	1.81×10^{-5}	4.5×10^{-7}
Ar	3.49×10^{-6}	7.7×10^{-8}
O_2	4.27×10^{-6}	6.4×10^{-8}
N_2	2.99×10^{-6}	8.1×10^{-9}
CH_4	0.70×10^{-6}	4.4×10^{-9}
CO_2	4.40×10^{-6}	5.3×10^{-7}

D in cm^2/s and P in $cm^3(STP)cm/cm^2$ s atm.

The permeability, which can be estimated by $P = DS$, is listed in Table II. Since the values of P significantly vary with the size of the gases, these gases could be precisely separated using the membrane of the α form crystal.

3.4 Application to smart membrane

A membrane, in which precisely controlled molecular cavities are embedded, is a candidate for a "smart membrane" [16]. The membrane would realize a significantly high permselectivity, which could be obtained neither by conventional rubbery, nor amorphous glassy, nor macroscopic porous membranes. The δ_e form may be used as the smart membrane, by which chemically alike molecules, such as the *p*- and *m*-xylene, can be separated, utilizing the slight difference between the structure of the molecular cavity and that of the guests [13]. Trace amounts of aromatic molecules may also be absorbed from contaminated water by the membrane. The large size environmental hormones may be strictly separated because the larger gases show a significantly high solubility in the molecular cavity. The diffusion process in the δ_e form is governed by the narrow channels between the large cavities and is controlled by the temperature. Gases such as carbon dioxide and natural gas may be stored in the δ_e form, in combination with gating of the permeation paths by pinpoint heating. In the α form, the diffusion process is governed by the fast one-dimensional gas transport. If an oriented single crystal of the α form could be obtained, it could be used as a high-performance gas separation membrane.

4. CONCLUSIONS

The nanoscale cavity structure in the polymorphs of crystalline s-PS was analyzed in detail. The cavity structure in the δ_e form can suitably be called a molecular cavity. The large individual holes with a regular shape and size are connected in an orderly manner by narrow channels. Another class of cavity structures, a molecular capillary, was found in the α form. The diffusion behavior and solubility of gases in these crystals were clearly interpreted in terms of the difference in the cavity structures. The hypothesis for the structure and connectivity of cavities derived from the present simulation is consistent with several experimental observations. The novel concept of the molecular cavity will be a breakthrough in the precise and effective separation of substances, e.g., carbon dioxide, hydrocarbons, and environmental hormones.

ACKNOWLEDGMENTS

This work was supported by a Grant-in-Aid for Scientific Research on Priority Areas (No.13133203) from the Ministry of Education, Culture, Sports, Science and Technology, Japan.

REFERENCES

[1] O. Greis, Y. Xu, T. Asano, and J. Petermann, *Polymer*, **30**, 590-4 (1989).
[2] G. Guerra, V. M. Vitagliano, C. de Rosa, V. Petraccone, and P. Corradini, *Macromolecules*, **23**, 1539-44 (1990).
[3] C. de Rosa, G. Guerra, V. Petraccone, and P. Corradini, *Polymer J.*, **23**, 1435-42 (1991).
[4] Y. Chatani, Y. Shimane, Y. Inoue, T. Inagaki, T. Ishioka, T. Ijitsu, and T. Yukinari, *Polymer*, **33**, 488-92 (1992).
[5] Y. Chatani, Y. Shimane, T. Inagaki, T. Ijitsu, T. Yukinari, and H. Shikuma, *Polymer*, **34**, 1620-24 (1993).
[6] Y. Chatani, Y. Shimane, T. Ijitsu, and T. Yukinari, *Polymer*, **34**, 1625-29 (1993).
[7] C. de Rosa, *Macromolecules*, **29**, 8460-5 (1996).
[8] C. de Rosa, G. Guerra, V. Petraccone, and B. Pirozzi, *Macromolecules*, **30**, 4147 (1997).
[9] C. Manfredi, M. A. del Nobile, G. Mensitieri, G. Guerra, and M. Rapacciuolo, *J. Polym. Sci. Polym. Phys. Ed.*, **35**, 133-40 (1997).
[10] G. Guerra, C. Manfredi, P. Musto, and S. Tavone, *Macromolecules*, **31**, 1329-34 (1998).
[11] K. Tsutsui, Y. Tsujita, H. Yoshimizu, and T. Kinoshita, *Polymer*, **39**, 5177-82 (1998).
[12] G. Guerra, G. Milano, V. Venditto, P. Musto, C. de Rosa, and L. Cavallo, *Chem. Mater.*, **12**, 363-8 (2000).
[13] M. Sivakumar, Y. Yamamoto, D. Amutharani, Y. Tsujita, H. Yoshimizu, and T. Kinoshita, *Macromol. Rapid Commun.*, **23**, 77-9 (2002).
[14] K. Hodge, T. Prodpran, N. B. Shenogina, and S. Nazarenko, *J. Polym. Sci. Polym. Phys. Ed.*, **39**, 2519-38 (2001).
[15] Y. Tamai and M. Fukuda, *Polymer*, **44**, 3279-89 (2003).
[16] Y. Tsujita, unpublished.
[17] Y. Tamai and M. Fukuda, *Chem. Phys. Lett.*, **371**, 217-22 (2003).
[18] W. D. Cornell, P. Cieplak, C. I. Bayly, I. R. Gould, K. M. Merz, Jr., D. M. Ferguson, D. C. Spellmeyer, T. Fox, J. W. Caldwell, and P. A. Kollman, *J. Am. Chem. Soc.*, **117**, 5179-97 (1995).
[19] S. Nose *J. Chem. Phys.* **81**, 511-9 (1984).
[20] M. Parrinello and A. Rahman, *J. Appl. Phys.*, **52**, 7182-90 (1981).

(Received October 13, 2003; Accepted March 17, 2004)